

Results from LHCb: prompt V^0 production

Manuel Schiller^{*†}

Physikalisches Institut der Universität Heidelberg, Germany

E-mail: schiller@physi.uni-heidelberg.de

Preliminary results of an analysis which measures the K_S^0 production cross section in pp collisions at $\sqrt{s}=900$ GeV are presented, using data taken with the LHCb detector during December 2009. The measurement is performed double-differentially in a p_T range from 200 to 1600 MeV and a range from 2.5 to 4 in rapidity y . The result is compared to predictions made with different tunes of the PYTHIA generator.

XVIII International Workshop on Deep-Inelastic Scattering and Related Subjects

April 19 -23, 2010

Convitto della Calza, Firenze, Italy

^{*}Speaker.

[†]On behalf of the LHCb collaboration

1. Data taking conditions

The data sample consists of 13 runs taken with the LHCb detector [1] from December 11, 2009 to December 15, 2009. Low intensity beams were collided for the first time in stable conditions at a centre-of-mass energy of 900 GeV. All components of the LHCb detector were turned on, and the dipole magnet ran at nominal field strength. However, due to the larger aperture required by the low energy beams, the vertex detector (VELO) was retracted by 15 mm with respect to the nominal operating position. A minimum bias calorimeter trigger required at least one cluster in the hadronic calorimeter with a transverse energy above 240 MeV and at least three hits in the Scintillating Pad Detector (6016 cells in total) in front of the calorimeters.

The integrated luminosity of $\mathcal{L} = 6.8 \pm 1.0 \mu\text{b}^{-1}$ was determined using a direct beam profile measurement using the VELO and the bunch currents supplied by the LHC, details in [2] and [3]; for this, an additional trigger based on information of the Pile-Up System was used, designed to fire on interactions of proton beams with residual gas in the beam pipe.

2. Analysis strategy

We reconstruct K_S^0 candidates in the $\pi^+\pi^-$ mode as function of transverse momentum $p_T = \sqrt{p_x^2 + p_y^2}$ and rapidity $y = \frac{1}{2} \ln \frac{E+p_z}{E-p_z}$ where (E, \vec{p}) is the four-momentum in the rest frame of the pp collision. Due to the relatively long lifetime of the K_S^0 and the non-standard VELO position, only a small fraction of K_S^0 decay products have VELO information. Therefore, we focus on K_S^0 candidates formed from so-called downstream tracks which have hits in the tracking stations directly in front of and behind the dipole magnet (TT and T stations, respectively), ignoring any VELO hits.

For each bin (i, j) in p_T and y , the partial inclusive K_S^0 production cross section is calculated using $\sigma_{ij} = \frac{N_{ij}}{\mathcal{L} \epsilon_{ij}^{\text{trig}} \epsilon_{ij}^{\text{reco}}}$ where N_{ij} is the observed signal yield in the respective bin in data, and $\epsilon_{ij}^{\text{trig}}$ and $\epsilon_{ij}^{\text{reco}}$ are the trigger and reconstruction efficiencies in the bin in question. The exact definition and measurement of these efficiencies is described in more detail in section 6. We do not separate the contributions from K_S^0 produced in diffractive and non-diffractive processes.

3. Selection

The selection consists of track quality cuts and exploits the K_S^0 lifetime, requiring the K_S^0 to point back to the primary vertex (PV) while its daughters must not originate there. To become independent of the PV reconstruction efficiency, we take the point $(0, 0, z)$ as PV which is closest to the reconstructed flight path of the K_S^0 . A detailed overview of selection cuts is given in Table 1.

4. Beam gas subtraction

Data taken in 2009 have some contamination by events in which one of the protons interacts with one of the residual gas atoms left inside the beam vacuum. To remove this contribution, each distribution is plotted separately for events in which only one beam has a filled bunch in LHCb (so-called ‘beam-empty’-events, any interaction seen must be due to beam gas) and events for which

cut	value
π momentum	< 2 GeV
π transverse momentum	< 50 MeV
π track χ^2/ndf	< 25
π impact parameter wrt. PV	> 3 mm
K_S^0 decay vertex χ^2/ndf	< 25
K_S^0 decay vertex z	< 2200 mm
$ z $ of PV	< 150 mm
$\cos(\theta_{\text{pointing}})$	> 0.99995
$c \times (K_S^0 \text{ proper time}) (ct)$	> 5 mm

Table 1: K_S^0 selection requirements. We take the point $(0,0,z)$ on the z axis as primary vertex (PV) which is closest to the reconstructed flight path of the K_S^0 . θ_{pointing} is the angle between the reconstructed momentum of the K_S^0 and the vector joining PV and K_S^0 decay vertex.

both beams have filled bunches in LHCb (containing either a pp collision or a beam gas interaction). Using the ratio of events outside the luminous region (primary vertex $z < -0.2$ m, see Figure 1), one can derive a normalisation factor $\beta = 0.92 \pm 0.02$ for the ‘beam-empty’ events which allows to statistically subtract the beam gas contribution ($< 1.5\%$ of all selected candidates) according to $N_{pp} = N_{bb} - \beta N_{be}$. Henceforth, all distributions shown have their beam gas contribution subtracted.

5. Signal extraction

Signal extraction is done using a binned maximum likelihood fit. A double Gaussian with a linear background is used to describe the $\pi^+\pi^-$ invariant mass distribution¹. Figure 2 shows the fits for all bins in p_T and y , Table 2 lists the extracted yields in each bin. Of all candidates passing the selection, we obtain 3811 ± 83 signal candidates in data, with a mean mass of 497.0 ± 0.2 MeV which is close to the known K_S^0 mass of 497.6 MeV [4]. The Gaussian resolutions are 6.1 ± 0.9 MeV for 40 % of the signal and 12.7 ± 1.3 MeV for the remainder. To assess fit stability and estimate systematic uncertainties, the fit model is varied (exponential as background model), and fitted signal yields in simulation are compared to Monte Carlo truth.

6. Efficiency determination

To measure efficiencies, we use a sample of simulated single pp collisions generated using

¹If the widths of both Gaussians are very similar, one Gaussian dominates or if there is too little statistics to reliably fit a double Gaussian, a single Gaussian is used instead.

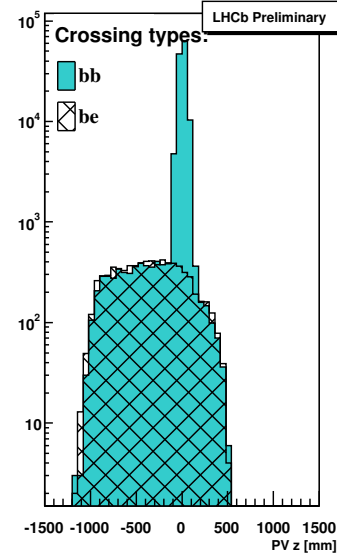


Figure 1: The distribution of the primary vertex z component for beam-beam (solid) and beam-empty (hatched) bunch crossings allows to derive the relative normalisation $\beta = 0.92 \pm 0.02$ outside the luminous region ($z < -0.2$ m).

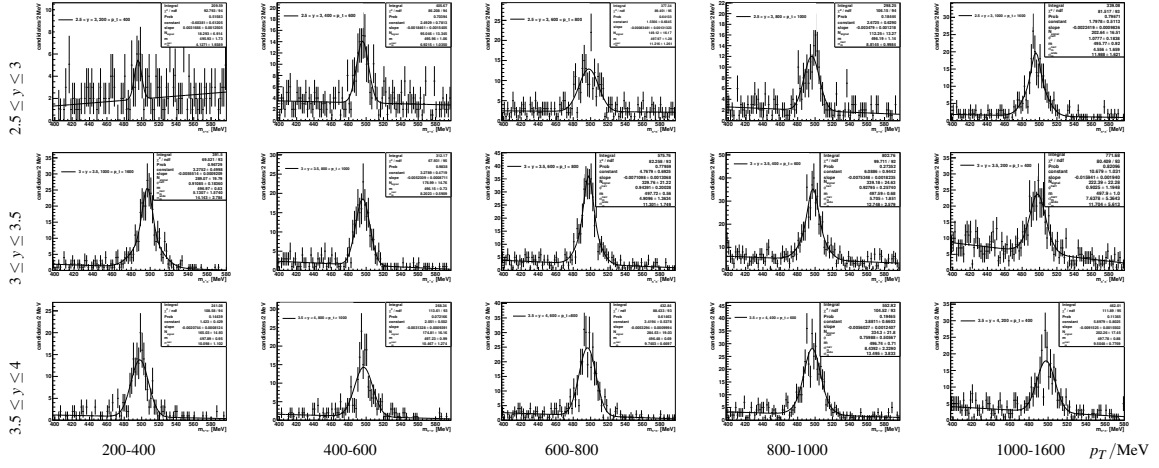


Figure 2: Fits to mass distributions of K_S^0 candidates in bins of p_T and y . The points are beam-gas subtracted data, the curve is the fit described in the text.

p_T [GeV]	$2.5 \leq y \leq 3.0$	$3.0 \leq y \leq 3.5$	$3.5 \leq y \leq 4.0$
0.2 – 0.4	18 ± 7	222 ± 22	202 ± 17
0.4 – 0.6	95 ± 13	339 ± 25	334 ± 22
0.6 – 0.8	149 ± 16	330 ± 21	285 ± 19
0.8 – 1.0	112 ± 13	177 ± 15	175 ± 16
1.0 – 1.6	203 ± 17	289 ± 20	165 ± 15

Table 2: Uncorrected K_S^0 yields and their associated statistical uncertainty in bins of p_T and y as extracted from the mass fits.

PYTHIA 6.4 [5]² and GEANT. Detector response has been tuned to reproduce test beam results. As the final alignment precision has not yet been reached³, one loses hits in data due to residual misalignments. To mimic this effect in the simulation, we measure the hit finding efficiency (fraction of cases in which a hit expected to be on a track based on track parameters and detector geometry is actually found on that track) in data and in simulation per tracking subdetector and layer. We then randomly set a flag on hits in simulation to have them ignored by the pattern recognition and all subsequent processing stages such that the hit finding efficiencies agree after the procedure. A sample of simulated data treated in this way is used to determine all efficiencies. Systematic errors for this procedure are assigned by observing the variation over phase space of the fraction of average number of hits per track in data over the corresponding average in the simulation.

6.1 Reconstruction efficiency

We define the reconstruction efficiency as $\epsilon_{ij}^{\text{reco}} = M_{ij}^{\text{obs}} / M_{ij}^{\text{gen}}$ where M_{ij}^{obs} is the number of observed signal candidates in the Monte Carlo simulation with reconstructed p_T and y inside the bin in question (using the same signal extraction procedure as in data), and M_{ij}^{gen} is the number

²The generated events include soft diffractive events, and the signal reconstruction efficiency is similar for diffractive and non-diffractive events. For a detailed description of which process types are included, see [6].

³Due to the forward geometry of LHCb, alignment with cosmic muons is only possible for very few subdetectors and statistics is rather limited.

of true K_S^0 mesons produced in prompt pp collisions with true p_T and y inside the given bin. This definition of reconstruction efficiency includes reconstruction and selection efficiencies and corrections due to secondary interactions of K_S^0 in material, absorption, $K_S^0 \rightarrow \pi^+\pi^-$ branching fraction, decay in flight and secondary interaction of decay products, non-prompt K_S^0 production and finite resolution of reconstructed p_T and y .

6.2 Trigger efficiency

Using two uncorrelated classes of events (events known to have been triggered by K_S^0 daughters and events known to have been triggered by other tracks in the event), the trigger efficiency is measured relative to offline selected K_S^0 in bins of reconstructed p_T and y . Because the data sample does not have sufficient statistics to measure the trigger efficiency in two dimensions as function of p_T and y , we use simulated events to do this measurement⁴. One can then project the efficiencies measured in simulated events along p_T or y and compare these one-dimensional distributions to the corresponding distributions determined on data (statistics is sufficient for that purpose). Trigger efficiencies range from 96 % to 99 %, and data-Monte Carlo agreement is quite good. The remaining discrepancy is used to estimate systematic uncertainties.

7. Systematic studies

Various studies have been performed to estimate the size of systematic uncertainties. Apart from those already mentioned in the text, these include systematics on stability of the selection (by releasing one cut at a time), fit stability, corrections due to non-prompt K_S^0 , beam gas subtraction and branching ratio uncertainties. The largest effects on the cross section are due to luminosity (15 %), tracking efficiencies (8 %), fit stability (4 %), selection (3 %) and trigger (2 %) efficiencies, all other effects being below the percent level.

8. Results

Table 3 gives the measured partial cross section, which are also plotted in Figure 3 with the results divided by the respective bin area $\Delta p_T \Delta y$. These are compared to predictions obtained by various tunes of PYTHIA 6.4:

- the standard settings currently used by LHCb, including soft diffraction as described by PYTHIA 6.4 (black dashed curve; see [6] for details)
- the standard LHCb settings excluding diffractive events (black continuous curve)
- the “Perugia 0” tune [7], which does not include diffraction (pink curve)

In general, the predictions agree tolerably well with the data (given that there are no previous measurements in this kinematic region to tune models to), although K_S^0 production at higher values of p_T seems to be underestimated. The analysis is being refined and finalised; in particular, an

⁴The sample of simulated events is reweighted to reproduce the observed downstream track multiplicity distribution in data before the trigger efficiencies can be extracted (the multiplicity in data is slightly higher): Intuitively, having more tracks in the event increases the chance to trigger on a track which is not from the signal decay. Indeed, trigger efficiencies in data are 1-2 % higher than in simulated events before the reweighting.

additional analysis using K_S^0 daughters with VELO information provides a cross-check.

References

- [1] The LHCb Collaboration, *The LHCb Detector at the LHC*, Journal of Instrumentation, **2008 JINST 3** S08005
- [2] V. Balagura, *Luminosity measurement at LHCb*, talk at *Moriond QCD and High Energy Interactions*, 2010
- [3] D.A. Moran, *Luminosity measurements at LHCb*, in proceedings of *XVIII International Workshop on Deep-Inelastic Scattering and Related Subjects*, PoS(DIS 2010)082
- [4] C. Amsler et al. (Particle Data Group), *Review of Particle Physics*, Physical Letters **B 667**, 1 (2008)
- [5] T. Sjöstrand, S. Mrenna and P. Skands, *PYTHIA 6.4: Physics and manual*, JHEP **05** (2006) 026 [arXiv:hep-ph/0603175]
- [6] The LHCb Collaboration, *Prompt K_S^0 production in pp collisions at $\sqrt{s} = 900$ GeV*, CERN-LHCb-CONF-2010-008
- [7] P. Skands, *The Perugia tunes*, [arXiv:0905.3418v1]

p_T [GeV]	$2.5 \leq y \leq 3.0$	$3.0 \leq y \leq 3.5$	$3.5 \leq y \leq 4.0$
0.2 – 0.4	$0.31 \pm 0.13 \pm 0.06$	$0.61 \pm 0.06 \pm 0.11$	$0.54 \pm 0.05 \pm 0.10$
0.4 – 0.6	$0.52 \pm 0.08 \pm 0.10$	$0.55 \pm 0.04 \pm 0.10$	$0.57 \pm 0.04 \pm 0.11$
0.6 – 0.8	$0.44 \pm 0.05 \pm 0.09$	$0.40 \pm 0.03 \pm 0.07$	$0.37 \pm 0.03 \pm 0.07$
0.8 – 1.0	$0.20 \pm 0.03 \pm 0.03$	$0.19 \pm 0.02 \pm 0.03$	$0.24 \pm 0.03 \pm 0.05$
1.0 – 1.6	$0.26 \pm 0.03 \pm 0.05$	$0.29 \pm 0.03 \pm 0.05$	$0.26 \pm 0.03 \pm 0.05$

Table 3: Prompt K_S^0 production cross section in mb measured in bins of p_T and y . The first uncertainty given is the statistical one, the second corresponds to the systematic uncertainties.

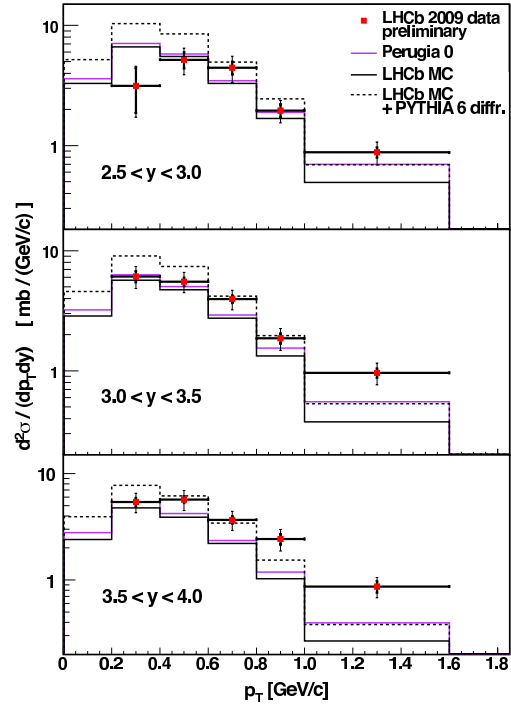


Figure 3: Differential prompt K_S^0 production cross section in pp collisions at $\sqrt{s} = 900$ GeV as function of p_T in three rapidity bins. The thick (thin) error bars correspond to the statistical (total) uncertainties. Predictions from different PYTHIA generator tunings (solid/dashed histograms) are shown for comparison (see text).